

Review

Optical coherence tomography: a novel technique for the study of tissue microcirculation

Junji Seki

Department of Biomedical Engineering, National Cardiovascular Center Research Institute, Suita, Osaka 565-8565, and CREST, Japan Science and Technology Agency, 4-1-8 Honcho Kawaguchi, Saitama 332-0012, Japan

Background: Three-dimensional (3D) observation techniques are useful for understanding organ microcirculation. Optical coherence tomography (OCT) is one of the 3-D imaging techniques and is increasingly applied for tissue microcirculatory studies.

Objective: This article reviews the current and prospective usages of OCT in microcirculation.

Methods: OCT is an optical technique to obtain tomographic images of highly scattering media like living tissues by means of coherence gating, whose spatial resolution is down to 10 μm . It is also capable of obtaining velocity profiles of blood flow by use of Doppler frequency shift (Doppler OCT).

Results: The OCT technique has been applied for observation of microvessels in rat skin, hamster dorsal skin, rat brain etc. Small microvessels down to 20 μm have been detected with the aid of Doppler OCT. Doppler OCT also revealed that the blood flow in microvessels is a quasi-steady laminar flow. The OCT signal from the cerebral cortex was found to change following neural activation, probably reflecting the functional hyperemia.

Conclusion: The OCT technique combined with Doppler OCT technique has a great potential for *in vivo* observation of 3-D structures of microvessels and blood flow distribution. Further OCT is expected to be a depth-dependent imaging tool for the study of brain function.

Keywords: Doppler OCT, functional brain imaging, optical coherence tomography, velocity profile, velocity pulsation.

The optical microscope is generally used for *in vivo* observation of microcirculatory systems of animals, including microvessels, blood cells, lymphatic vessels, and small structures of other tissues and cells surrounding microvessels. However, the optical microscope can be applied only to microvessels buried in thin transparent tissues or organ surfaces because the living tissue is a strong scattering medium for visible light. Hence the subjects of microcirculatory studies have been mostly limited to mesentery, omentum, cremaster muscle, pia mater etc, whose vascular distribution is almost 2-dimensional. In order to understand the transport processes of nutrients including oxygen, which are one of the most important functions of microcirculatory system, it is necessary to get 3-dimensional information on the conformation

of vascular trees traveling within organs as well as the cross-sectional shape of each vessel.

Ultrasonography, magnetic resonance imaging (MRI) and positron emission tomography (PET) can image living tissues to a depth of several tens of centimeters, and they are applied to viewing internal structure of organs. The spatial resolution of ultrasonography is several hundreds μm , that of MRI is around mm, and that of PET is even larger, which are too low to resolve microvessels whose diameter is less than 100 μm . On the other hand, the confocal laser scanning microscope (CLSM) and multi-photon microscope have much better spatial resolution, but their penetrating depth is only around 100 μm [1]. Optical coherence tomography (OCT), which was developed more recently than those techniques, is capable of viewing living tissues with spatial resolution around 10 μm and penetrating depth of up to a few mm [2]. Both the spatial resolution and penetrating depth are intermediate between MRI and CLSM. Since a system of OCT for examination of

eyegrounds is commercially available, most of the clinical application of OCT has been done in ophthalmology [3]. Experimentally, it has been applied not only to observation of structural organization of the dermis [4], esophagus and trachea [5], the vascular wall of large arteries [6], intestine [7], but also to the high-resolution observation of various types of living cells [8-10].

Since the typical OCT system has a spatial resolution around $10\ \mu\text{m}$ as indicated above, it has also been used for observing microvessels in living tissues. Moreover, it is capable of measuring blood flow velocity in microvessels by means of detecting Doppler shift frequency, similar to the technique of Doppler ultrasound [11]. In this article, the application of OCT to microcirculatory studies is discussed including our studies on nervous tissues of the cerebral cortex.

Optical coherence tomography

OCT is a technique for visualizing internal structure of turbid media like living tissues up to a few mm depth with around $10\ \mu\text{m}$ resolution by utilizing an incoherent light source, usually infrared. The concept of detecting position by use of a low-coherence light source was first introduced by Takada of NTT [12]. A practical system capable of measuring living tissues has been developed by the Fujimoto group at the Massachusetts Institute of Technology (MIT) [2].

The operational principle of OCT is often compared with B-mode ultrasonic imaging (ultrasonography). In ultrasonography, a short pulse

of ultrasound is transmitted into a tissue and then the signal that is reflected from the specific position (depth) inside the tissue is discriminated by a time window with the delay time corresponding to the depth. Such method of discriminating the depth of signal source is called "time gating". On the other hand, in OCT, depth discrimination is effected by using the coherency of light, which is called "coherence gating". In actual settings as shown in **Fig. 1**, incoherent light is split into two beams, one of which is transmitted into an object and the other on to a mirror. The light reflected from within the sample is interfered by that reflected from the reference mirror. Let us consider a special case where a strong scatterer is buried in the sample. Then, the intensity of the interference signal attains maximum when the optical path length of the sample beam from the light source to the scatterer is equal to that of the reference beam from the source to the mirror, and it damps rapidly as the path length difference increases larger than the coherence length. The maximum value of the interference signal is proportional to the light intensity reflected from the scatterer. In actual cases where many scatterers distribute in the sample, the longitudinal distribution of light intensity reflected from within the sample can be obtained by scanning the mirror in the direction of light axis. **Figure 1** shows a schematic of a typical fiber-optic based OCT system of Huang et al. [2]. In order to obtain a two-dimensional distribution of reflected light intensity (cross-sectional image), lateral scan is performed by translating the sample stage in the direction perpendicular to the sample beam axis.

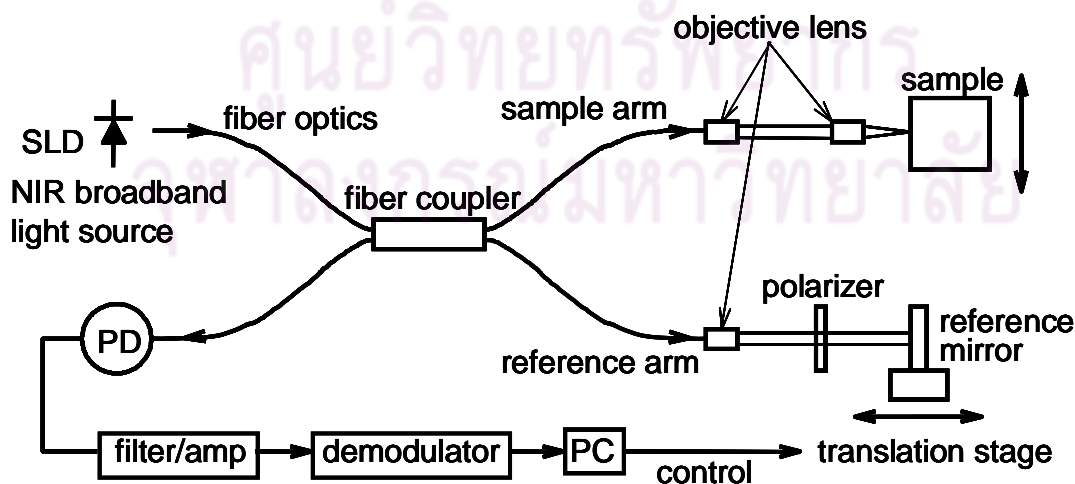


Fig. 1 Typical configuration of a fiber-optic based OCT (optical coherence tomography) system. PD: photo detector, PC: personal computer.

Light sources used in OCT include superluminescent diodes (SLD), light emitting diodes (LED) and short pulse lasers, whose central wavelength is in the near infrared region (800-1500 nm) and spectral bandwidth ranges from a few tens to several hundreds of nm. The longitudinal depth resolution of the OCT is in the order of the coherence length of the light source. Since the coherence length is inversely proportional to the spectral bandwidth, the spatial resolution of OCT becomes higher as the light source develops a broader spectral bandwidth. For example, the coherence length is 32 μm for the light source with 810 nm central wavelength and 20 nm spectral bandwidth, and it is 11 μm for 940 nm central

wavelength and 80 nm bandwidth. The actual longitudinal resolution is modulated by the refractive index of the medium and the method of signal processing. For example, the full width at half maximum (FWHM) of the OCT signal is estimated about 16 μm in a living tissue for a SLD with 810 nm central wavelength and 20 nm spectral bandwidth [13]. The OCT system using a very short pulse laser whose spectral bandwidth is 350 nm attains an axial resolution of 2-3 μm [9]. The lateral resolution is estimated as the waist diameter of the sample beam, which is dependent on the original beam width and the focusing length of the objective lens.

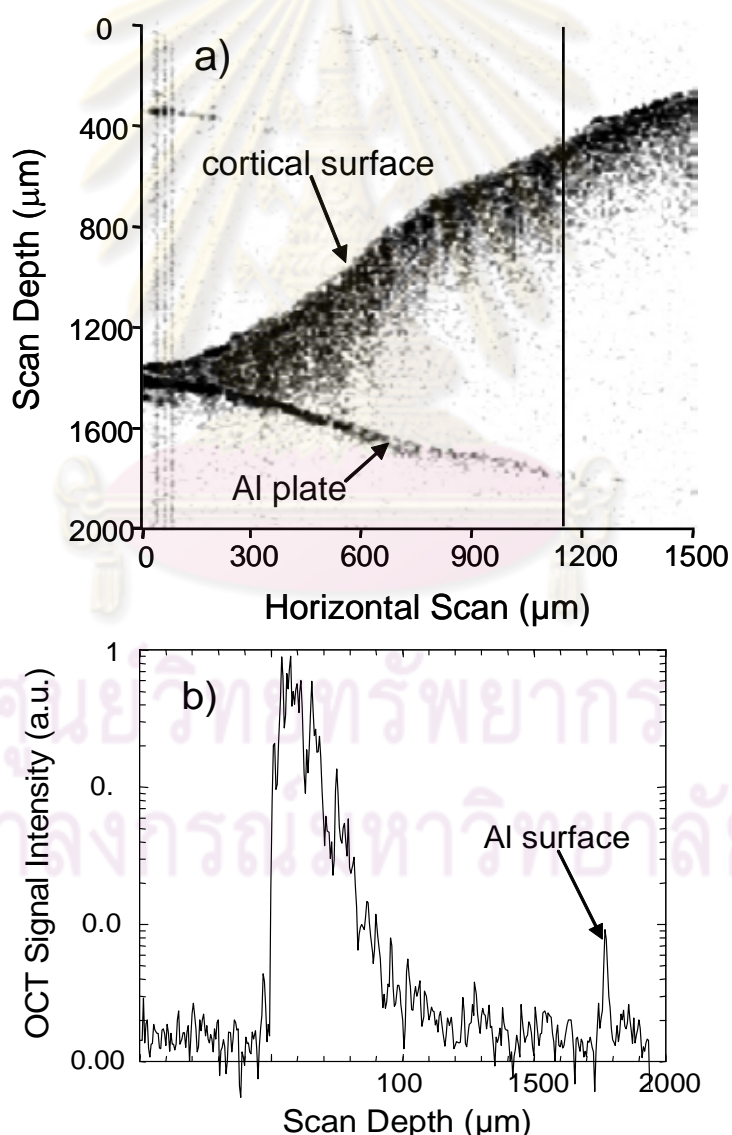


Fig. 2 (a) OCT image of a wedge-shaped slice of rat cerebral cortex placed on an aluminum plate [13]. The central wavelength of the light source (SLD) is 940 nm, and the bandwidth is 80 nm. Scan depth is expressed in the unit of optical path length. (b) Distribution of OCT signal intensity along the vertical line shown in **Fig. 2** (a).

The penetrating depth of OCT in living tissues depends on the power of the light source, wavelength and beam diameter as well as the optical property of the tissue. **Figure 2** shows an example of an in vitro OCT observation of wedge-shaped slice of rat brain cortex placed on an aluminum plate. As shown in **Fig. 2 (b)**, the signal intensity is maximum at the cortical surface and it decreases exponentially with depth. The peaks represent the internal structure of the tissue. It is noted that the reference beam is transmitted in the air, while the sample beam is transmitted in the tissue. As a result, the optical path length of the sample beam is elongated by the factor of the refractive index of the tissue. Therefore the aluminum surface, that was set horizontally, appears curved under the cortical slice. The actual position of the sampling point inside the tissue is determined by

taking this effect into account. Conversely, the refractive index of the sample can be estimated using this effect [13]. The aluminum surface is clearly seen at a depth of about 1.3 mm on the scale of the optical path length (**Fig. 2 (b)**), that corresponds to 0.93 mm in the actual scale.

Observation of microvessels with OCT

There are very few examples of direct observation of microvessels with OCT. Some possible reasons are as follows. The spatial resolution of OCT (around 10 μm) is somewhat insufficient for observation of microvessels with diameter of several tens of μm . Secondly, the frequency of OCT signal from red cells flowing in microvessels might shift due to the Doppler effect and the signal may turn away from the bandwidth of signal demodulation. As a result, the

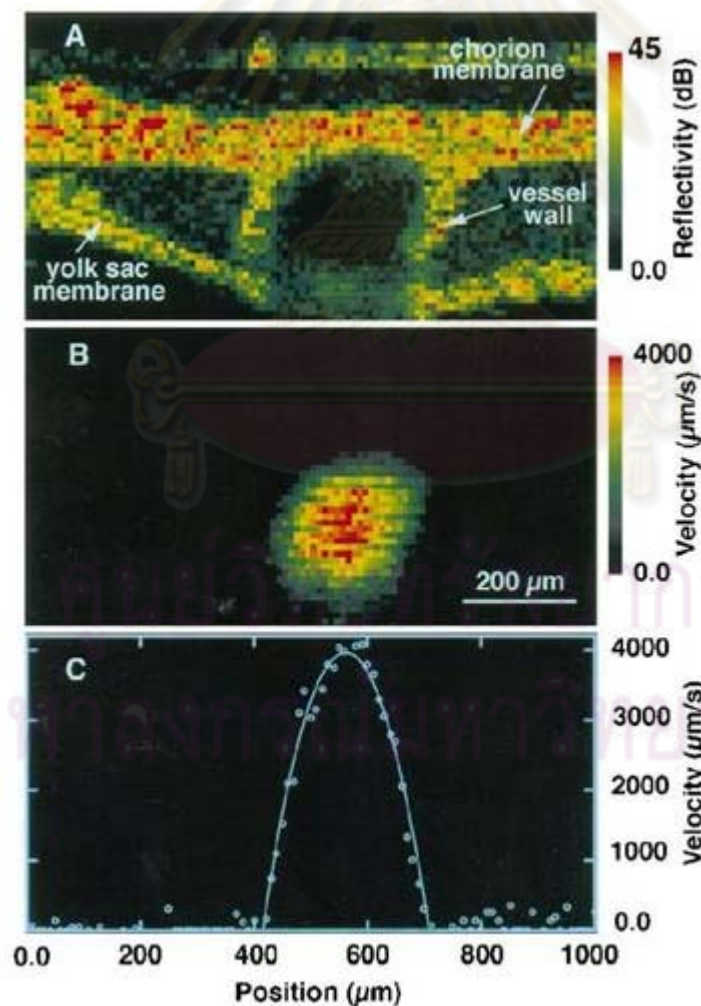


Fig. 3 **A:** Structural image of a chick chorioallantoic membrane (CAM) obtained with optical Doppler tomography [11]. **B:** Two-dimensional distribution of blood flow velocity in the CAM vein. **C:** Velocity distribution along the horizontal diameter of the vein shown in **Fig. 3B**.

vessel lumen cannot be visualized by OCT in such a case. In addition, since the blood is a strong scatterer of light, the OCT signal from the tissue behind the blood stream is highly attenuated so that even the rear wall of the microvessel may be concealed, which is called “shadow casting effect” [14, 15]. **Figure 3A** shows an OCT image of a microvessel in the chorioallantoic membrane of chicken egg obtained by Chen et al. [11]. The ring-shaped image in the center of the figure is the vascular wall of a venule with about a 150 μm diameter. As described above, the vessel lumen is not imaged possibly due to the Doppler effect, and the OCT signal from the yolk sac underneath the venule is low due to the shadow casting effect. On the contrary, velocity distribution inside the vessel can be obtained by measuring the Doppler shift frequency as shown in **Figs. 3B and 3C**. Especially **Fig. 3C** shows that the velocity distribution along a diameter coincides well with the parabola (solid line),

which indicates that the blood flow in the venule is a fully developed laminar flow (Hagen-Poiseuille flow). The same OCT system was also applied to rat skin microvessels [11]. The structural OCT image and velocity distributions are shown in **Fig. 4**. It is difficult to distinguish the arteriole of 20-30 μm diameter only from the structural image that may appear in the upper-right part of **Fig. 4A**. However, 2-dimensional velocity distribution (**Fig. 4C**) helps us to detect the vessel and further to measure its diameter.

In another example shown in **Fig. 5**, microvessels in hamster dorsal skin were observed by a similar OCT system utilizing the Doppler signal [16]. **Figure 5a** shows the 2-dimensional distribution of blood flow velocity that was obtained by scanning from the subcutaneous side of the dorsal skin flap. Three vessels appear in the figure with blood flow in the opposite directions. The 3-dimensional configuration of the vessels reconstructed from the Doppler OCT

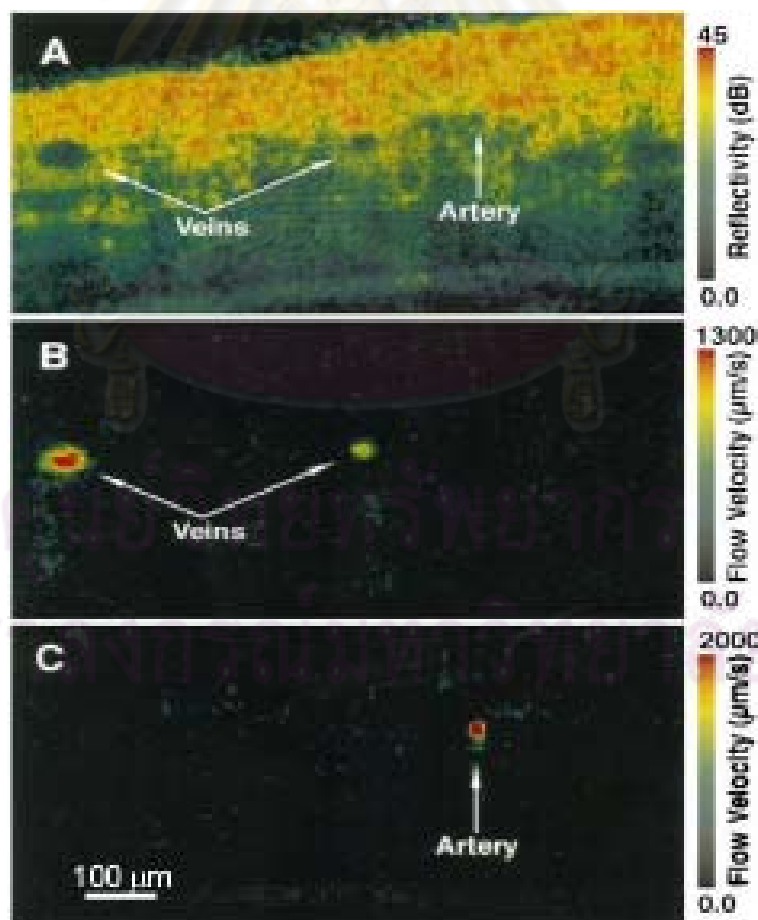


Fig. 4 **A:** Structural image of a rat skin including an artery and veins obtained with optical Doppler tomography [11]. **B:** 2-D distribution of velocity in the direction into the page. **C:** 2-D distribution of velocity in the direction out of the page.

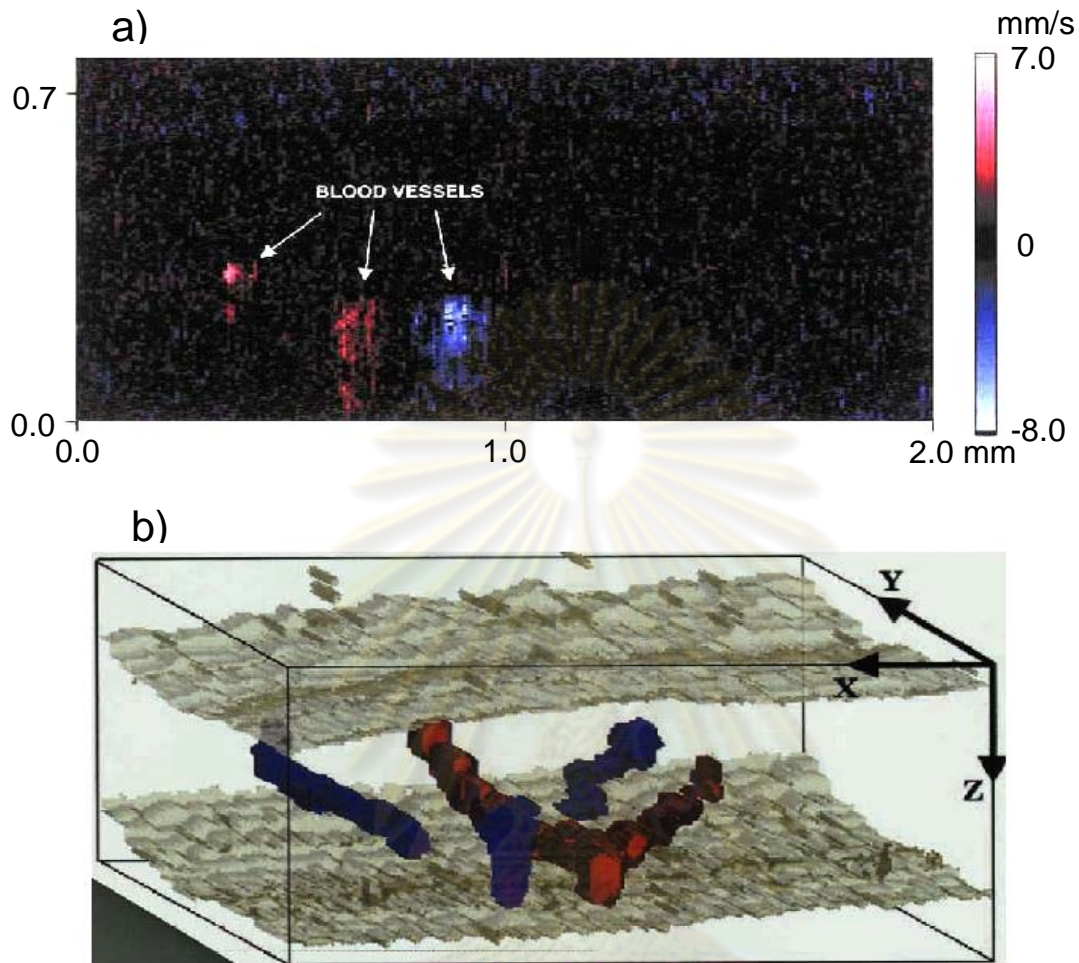


Fig. 5 a) 2-D distribution of blood flow velocity in a hamster dorsal skin flap model [16]. Red and blue colors show the flow direction away from and toward the probe, respectively. b) 3-D reconstruction of microvessels superposed on the OCT image of the epi- and sub-dermal surfaces.

images is shown in **Fig. 5b** together with the OCT structural images of the epi- and sub-dermal surfaces of dorsal skin flap. Branching, running and topology of the vessels are well recognized from the 3-D view. The Doppler OCT image such as **Fig. 5a** was obtained by off-line processing of the OCT signal, where it took several 10s sec to obtain the original 2-D OCT signal. The same research group developed a real time imaging system by achieving fast scan as well as hardware-based analog signal processing [17].

Application of OCT to cerebral microcirculation

The cerebral cortex is a tissue containing nerve cells and nerve fibers, and is a few mm thick. It consists of 6-layered structures in the depth direction and column structures with 0.5-1 mm diameter that are arranged on the cortical surface [18]. The column

structure is considered to be a functional unit of neural activity. Since the regional cerebral blood flow in microvessels is well coupled with the regional neural activity, which is called neuro-vascular coupling, it is interesting to investigate the structure and function of microvessels in cortical tissue down to the level of layers and functional columns. The characteristics of OCT match the thickness and the submillimeter scales of internal structures of the cerebral cortex.

Here, I will discuss a few of our recent studies of cerebral microcirculation using OCT. Our OCT system is a typical fiber-optic based system as shown in **Fig. 1**. The light sources are SLD's with central wavelengths of 813 and 940 nm, whose axial resolution is about 16 and 8.4 μm , respectively, and the beam spot diameter is about 14 μm . **Figure 6** shows an example of in vivo OCT image of somatosensory

cortex of the rat [13]. The boundary surfaces such as the dura, arachnoid membrane, and pial surface are well recognized, since the refractive index of the medium is largely different from that of either side of the interface. The cortical tissue can be imaged up to 1 mm in optical path length from the dura surface. Under the microvessels, however, the penetration depth was severely restricted, probably due to the shadow casting effect described earlier. **Figure 7**

shows another example of an OCT image of cerebral cortex whose dura was removed. The OCT signal intensity was very low in the vessel lumen for the pial arteriole seen in the central part of the figure, which is probably due to the Doppler effect written in the previous section. In addition, comparing **Figs. 6 and 7**, we note that the pial microvessels of the cerebral preparations with intact dura appear to float in the cerebrospinal fluid filling the subarachnoid space,

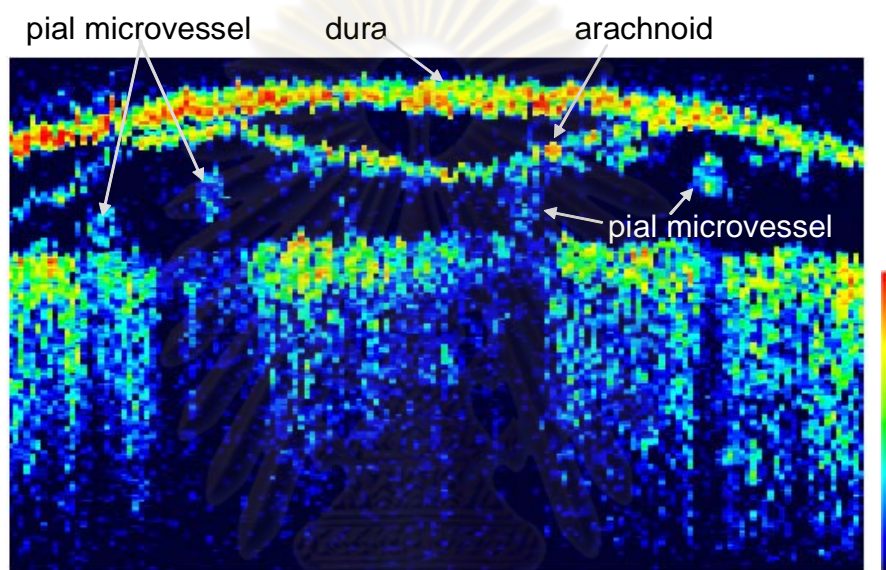


Fig. 6 *In vivo* OCT image of the rat cerebral cortex with intact dura [13]. The image covers 1.5 mm x 1 mm area, the vertical distance being expressed in units of optical path length.

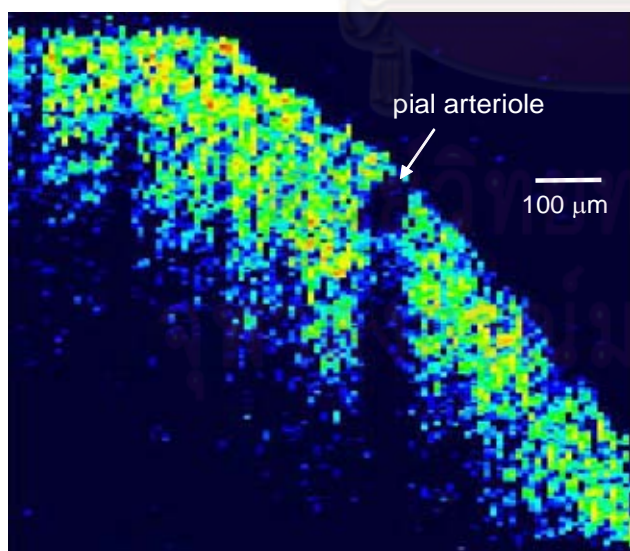


Fig. 7 *In vivo* OCT image of the rat cerebral cortex without dura [13].

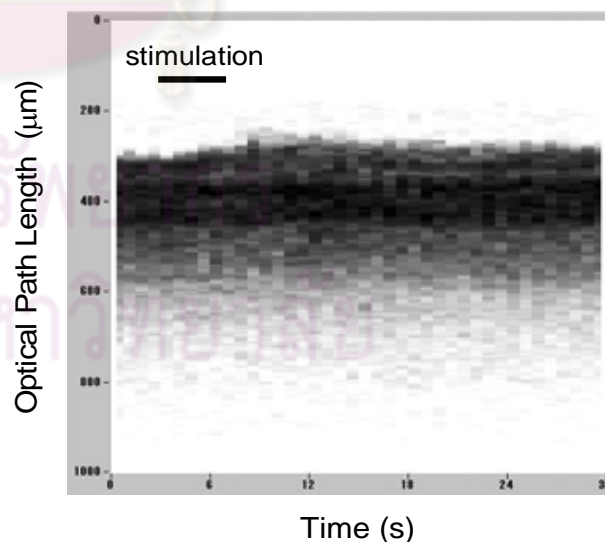


Fig. 8 Temporal change in OCT signal of the rat somatosensory cortex induced by electrical stimulation of the hind paw for the preparation without dura [13]. The stimulation was imposed between 3 and 7 second in the time course.

while they appear to be embedded in the cortical tissue in the cerebral preparations without dura [13].

There have been some reports that neural activation brings about changes in the OCT signal from the cerebral cortex [19]. In the cat visual cortex, visual stimuli evoked OCT signal changes dependent on the depth as well as on the area [19]. Aguirre et al. [20] found OCT signal change in the rat somatosensory cortex during electrical stimulation of forepaw. Although the causes of the OCT signal changes have not been determined yet, the results suggest the OCT technique can be applied to depth-resolved functional brain imaging (functional OCT). In the rat somatosensory cortex, we examined the effects of neural activation on the OCT signal [13, 21]. Temporal changes in OCT signal were measured following the

sensory stimulation of a hind paw. **Figure 8** shows an example of the results obtained in the cortical region corresponding to the hind paw. It showed a swelling of the cortical surface several seconds after the stimulus onset, and the region of swelling was restricted to a thin surface layer with less than several tens μm , which probably reflects the reactive hyperemia following the neuronal activation [13]. OCT signal changes were also detected in somatosensory and motor cortices of mice under the chronic ligation of sciatic nerve, which is a model of neuropathic pain [22]. OCT signal intensity increased in the hind paw area of the somatosensory and motor cortex contralateral to the ligated sciatic nerve.

Red cell velocity in pial microvessels and their changes following neural activation were determined

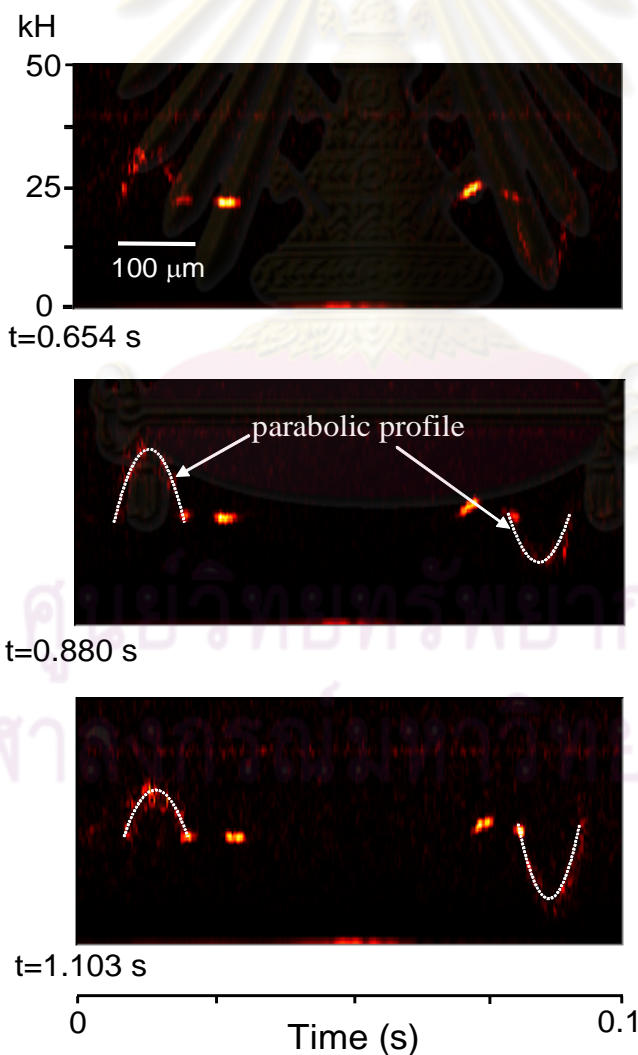


Fig. 9 Spectrograms of OCT signals obtained for a rat pial arteriole of 83 μm diameter during 0.1 second starting at three different times [21].

from the spectrogram of the OCT signal [21]. A remarkable feature of OCT used for flow velocity measurement is its depth resolution. The depth resolution of OCT is typically $10\ \mu\text{m}$, compared with several $100\ \mu\text{m}$ in the laser Doppler method [23], while the two-slit technique does not have depth resolution [24]. In addition, OCT the technique can provide cross-sectional velocity profiles of blood flow in microvessels with the same spatial resolution as in the tomographic imaging. In particular, the velocity profile along a diameter in the direction of the optical axis can be measured in a short time. **Figure 9** shows an example of spectrogram obtained for a pial arteriole by scanning the sampling point along the diameter perpendicular to the cortical surface. The frequency of about $21\ \text{kHz}$ corresponds to the Doppler frequency of the translational motion of the reference mirror. Arc-shaped protrusions from this line show the Doppler signal from the blood flow in the arteriole. It is because the scan direction was reversed that the arcs protrude upward and downward. It can be seen that the velocity profile kept a nearly parabolic shape, while the centerline velocity changed much. Such a large variation (up to 50% of the mean velocity) of centerline velocity reflects the cardiac pulsation. These facts indicate that the blood flow in the pial microvessels is a quasi-steady laminar flow, which is consistent with the flow expected in the case of a small Reynolds number and a small frequency parameter [25].

Figure 10 compares the velocity waveforms in the pial arteriole which perfuses the primary somatosensory area (S1) of the cerebral cortex, before and after electrical stimulation of the hind paw [21]. The velocity waveforms corresponded to the femoral artery pressure, indicating the velocity variation was brought about mainly by the heartbeats. In this example, the mean velocity increased by 13 %, while the amplitude of velocity pulsation increased by 40 % after stimulation than before stimulation. If the microvessels in the activated state simply dilate following neuronal stimulation, the mean velocity and the pulsatile amplitude ought to increase by the same ratio. Therefore such changes in the velocity impose a restriction on the mechanism of increases in the regional blood volume and blood flow (functional hyperemia).

Conclusion

Optical coherence tomography (OCT) is an evolving technique used for microcirculatory studies. Doppler OCT is unique in obtaining velocity profiles of blood flow in microvessels almost instantaneously. Therefore the OCT technique, especially useful when combined with Doppler OCT technique. It has a potential for *in vivo* observation of 3-dimensional structuring of microvessels and blood flow distribution in living tissues. It is also expected to offer a valuable means for the study of brain function, since the OCT signal from the cerebral cortex was found to show stimulus-induced changes in depth.

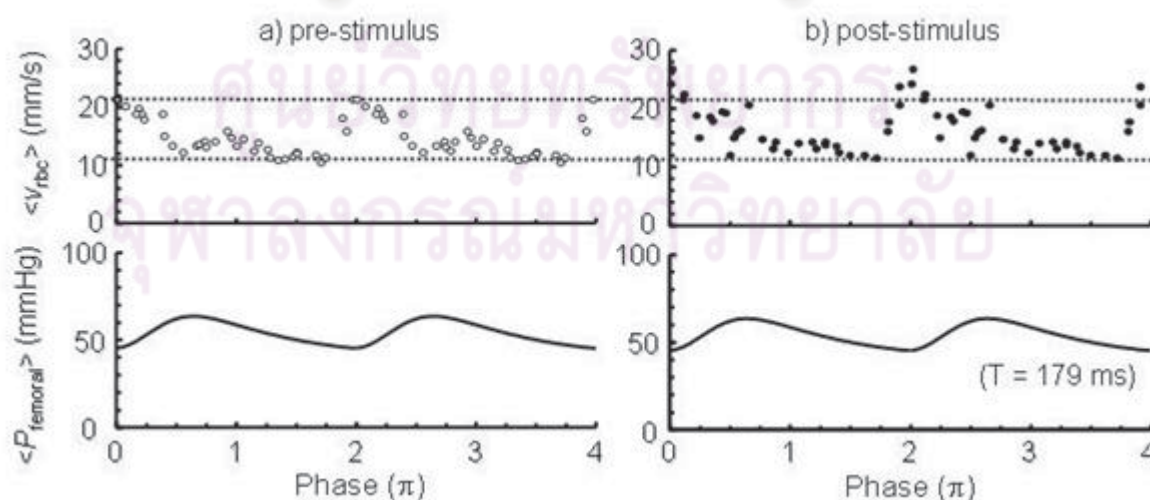


Fig. 10 Stimulus-induced changes of pulsatile waveforms of the red cell velocity in a pial arteriole between the periods before stimulation (a) and after stimulation (b) [21]. The stimulation was imposed electrically on the hind paw, and the arteriole perfused the corresponding somatosensory area of the cerebral cortex. The diameter of the arteriole was $120\ \mu\text{m}$. The dotted lines show the maximum and minimum velocities before stimulation.

Acknowledgement

This work was financially supported in part by Grants in Aid for Scientific Research No. 16591467 of Japan Society for the Promotion of Science, and by CREST of Japan Science and Technology Agency. The author has no conflict of interest to report.

References

1. Centonze VE, White JG. Multiphoton excitation provides optical sections from deeper within scattering specimens than confocal imaging. *Biophys J*. 1998;75:2015-24.
2. Huang D, Swanson EA, Lin CP, Schuman JS, Stinson WG, Chang W, et al. Optical coherence tomography. *Science*. 1991;254:1178-81.
3. Hee MR, Izatt JA, Swanson EA, Huang D, Schuman JS, Lin CP, et al. Optical coherence tomography of the human retina. *Arch Ophthalmol*. 1995;113:325-32.
4. Pan Y, Farkas DL. Noninvasive imaging of living human skin with dual-wavelength optical coherence tomography in two and three dimensions. *J Biomed Opt*. 1998;3:446-55.
5. Tearney GJ, Brezinski ME, Bouma BE, Boppart SA, Pitris C, Southern JF, et al. In vivo endoscopic optical biopsy with optical coherence tomography. *Science*. 1997;276:2037-9.
6. Tearney GJ, Yabushita H, Houser SL, Aretz HT, Jang IK, Schlendorf KH, et al. Quantification of macrophage content in atherosclerotic plaques by optical coherence tomography. *Circulation*. 2003;107:113-9.
7. Nishioka NS. Optical biopsy using tissue spectroscopy and optical coherence tomography. *Can J Gastroenterol*. 2003;17:376-80.
8. Boppart SA, Bouma BE, Pitris C, Southern JF, Brezinski ME, Fujimoto JG. In vivo cellular optical coherence tomography imaging. *Nature Med*. 1998;4:861-5.
9. Drexler W, Morgner U, Ghanta RK, Kartner FX, Schuman JS, Fujimoto JG. Ultrahigh-resolution ophthalmic optical coherence tomography. *Nat Med*. 2001;7:502-7.
10. Dubois A, Vabre L, Boccarda AC, Beaurepaire E. High-resolution full-field optical coherence tomography with a Linik microscope. *Appl Opt*. 2002;41:805-12.
11. Chen Z, Milner TE, Srinivas S, Wang X, Malekafzali A, Gemert MJ, et al. Noninvasive imaging of in vivo blood flow velocity using optical Doppler tomography. *Opt Lett*. 1997;22:1119-21.
12. Takada K, Yokohama I, Chida K, Noda J. New measurement system for fault location in optical waveguide devices based on an interferometric technique. *Appl Opt*. 1987;26:1603-6.
13. Satomura Y, Seki J, Ooi Y, Yanagida T, Seiyama A. In vivo imaging of the rat cerebral microvessels with optical coherence tomography. *Clin Hemorheol Microcirc*. 2004;31:31-40.
14. Boppart SA, Bouma BE, Brezinski ME, Tearney GJ, Fujimoto JG. Imaging developing neural morphology using optical coherence tomography. *J Neurosci Methods*. 1996;70:65-72.
15. Tadrous PJ. Methods for imaging the structure and function of living tissues and cells: I. Optical coherence tomography. *J Pathol*. 2000;191:115-9.
16. Barton JK, Izatt JA, Kulkarni MD, Yazdanfar S, Welch AJ. Three-dimensional reconstruction of blood vessels from in vivo color Doppler optical coherence tomography images. *Dermatology*. 1998;198:355-61.
17. Rollins AM, Yazdanfar S, Barton JK, Izatt JA. Real-time in vivo color Doppler optical coherence tomography. *J Biomed Opt*. 2002;7:123-9.
18. Bonhoffer T, Grinvald A. Optical imaging based on intrinsic signals, the methodology, In: Toga AW, Mazziotta JC, eds. *Brain Mapping*, New York:Academic Press; 1996, p. 55-97.
19. Maheswari RU, Takaoka H, Kadono H, Homma R, Tanifuji M. Novel functional imaging technique from brain surface with optical coherence tomography enabling visualization of depth resolved functional structure in vivo. *J Neurosci Methods*. 2003;124:83-92.
20. Azuirre AD, Chen Y, Fujimoto JG, Ruvinskaya L, Devor A, Boas A. Depth-resolved imaging of functional activation in the rat cerebral cortex using optical coherence tomography. *Opt Lett*. 2006;31:3459-61.
21. Seki J, Satomura Y, Ooi Y, Yanagida T, Seiyama A. Velocity profiles in the cerebral microvessels measured by optical coherence tomography. *Clin Hemorheol Microcirc*. 2006;34:233-9.
22. Ooi Y, Satomura Y, Seki J, Yanagida T, Seiyama A. Optical coherence tomography revealed in vivo cortical plasticity of adult mice in response to peripheral neuropathic pain. *Neurosci Lett*. 2006;397:35-9.
23. Seki J. Fiber-optic laser-Doppler anemometer microscope developed for the measurement of microvascular red cell velocity. *Microvasc Res*. 1990;40:302-16.
24. Baker Y, Wayland H. On-line volume flow rate and velocity profile measurement for blood in microvessels. *Microvasc Res*. 1974;7:131-43.
25. Seki J, Satomura Y, Ooi Y. Velocity pulse advances pressure pulse by close to 45° in the rat pial arterioles. *Biorheology*. 2004;41:45-52.